Green Frequency-Doubled Laser-Beam Propagation in High-Temperature Hohlraum Plasmas

C. Niemann,[1,2] R. L. Berger,[2] L. Divol,[2] D. H. Froula,[2] O. Jones,[2] R. K. Kirkwood,[2] N. Meezan,[2] J. D. Moody,[2] J. Ross,[2] C. Sorce,[2] L. J. Suter,[2] and S. H. Glenzer[2]

[1]*Electrical Engineering Department, University of California Los Angeles, Box 951594, Los Angeles, California 90095-1594, USA*
[2]*Lawrence Livermore National Laboratory, 7000 East Avenue, Livermore, California 94550, USA*

(Received 8 November 2007; published 29 January 2008)

We demonstrate propagation and small backscatter losses of a frequency-doubled (2ω) laser beam interacting with inertial confinement fusion hohlraum plasmas. The electron temperature of 3.3 keV, approximately a factor of 2 higher than achieved in previous experiments with open geometry targets, approaches plasma conditions of high-fusion yield hohlraums. In this new temperature regime, we measure 2ω laser-beam transmission approaching 80% with simultaneous backscattering losses of less than 10%. These findings suggest that good laser coupling into fusion hohlraums using 2ω light is possible.

DOI: 10.1103/PhysRevLett.100.045002 PACS numbers: 52.38.Hb, 52.38.Dx

The first laser driven hohlraum experiments [1,2] to demonstrate ignition and a burning plasma by inertial confinement fusion will employ blue (3ω) laser beams [3,4]. These beams, operating at a laser wavelength of $\lambda = 351$ nm, have been shown to effectively convert into soft x rays [5–7] suitable to heat a radiation cavity, i.e., a hohlraum, to radiation temperatures of 300 eV [8]. The soft x rays will be absorbed in the outer layers of the fusion capsule that is placed in the center of the hohlraum spherically compressing the deuterium-tritium fill by x-ray ablation pressure to densities and temperatures required for ignition by nuclear fusion. Experiments with blue beams that have investigated parametric laser-plasma instabilities by stimulated Brillouin scattering (SBS) and stimulated Raman scattering (SRS) have shown favorable scalings to ignition plasma conditions [9–11]. Recent findings with green laser beams [12–14], on the other hand, show that they may hold significant advantages for future ignition and high-gain or high-fusion yield experiments [15].

Figure 1 shows the design space for indirect drive inertial confinement fusion experiments [14] on the National Ignition Facility (NIF) [16]. The energy on target for green frequency-doubled light (2ω, 527 nm) is compared to frequency tripled (3ω, 351 nm) light. For a hohlraum coupling efficiency of 10% about 1.2 MJ of laser energy needs to be absorbed into the hohlraum to absorb 120 kJ into the fusion capsule, a value for which integrated radiation-hydrodynamic calculations show 10–20 MJ of fusion yield. For 3ω laser beams, the laser energy that can be delivered by the NIF exceeds this value by a factor of 1.5. The use of 2ω beams significantly enhances the design space; more laser energy to drive the hohlraum may be provided in excess of 3 MJ and the hohlraum coupling efficiency may be increased to 27%. The former is due to larger laser conversion efficiencies from the fundamental 1 μm wavelength of Nd:glass lasers to 2ω light. The latter extension stems from the use of larger hohlraums and larger ignition capsules for 2ω experiments [12,14]. Radiation-hydrodynamic calculations show that the extended design space will allow robust ignition hohlraum experiments employing large hohlraums with 50 MJ fusion yield or high-gain experiments with larger capsule with >120 MJ yield.

To achieve these conditions, the intense 2ω laser beams need to propagate through the large scale-length plasma formed inside the hohlraum in which laser beams may experience scattering losses from SRS and SBS.

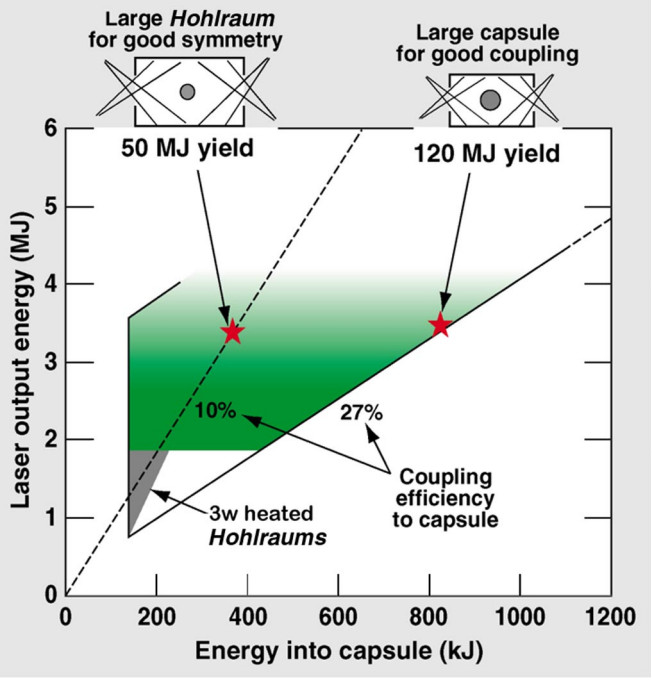

FIG. 1 (color online). The design space for ignition experiments on the NIF shows that experiments with 2ω beams will allow robust ignition or high-gain and high-yield fusion experiments due to larger possible laser energies and hohlraum coupling efficiencies.

Theoretical scalings [17,18] suggest that laser-plasma instabilities scale with $I\lambda^2$, where I is the intensity of the laser. This result suggests the use of significantly lower laser intensities for green than for blue beams. The increased size of the 2ω-driven hohlraums may employ larger laser entrance holes (LEH) allowing a beam intensity reduction from around 10^{15} W/cm^2 at 3ω to below 3×10^{14} W/cm^2 at 2ω. These hohlraums yield high plasma electron temperatures of $3 < T_e < 6$ keV where Landau damping is expected to efficiently reduce SRS and thus hot electron production that was observed in experiments at low electron temperatures [13,19,20].

In this Letter we present for the first time efficient propagation of an energetic 2ω laser beam in large scale-length plasmas ($\sim$2 mm) that approach ignitionlike hohlraum temperatures above 3 keV. These experiments employ a combination of beam smoothing techniques by continuous phase plates (CPP) [21], polarization smoothing (PS) [22], or smoothing by spectral dispersion (SSD) [23]. Applying PS and CPP yields 80% laser-beam transmission through the plasma with backscattering losses below 10%. The experiments further show that good propagation is accomplished by applying moderate laser-beam intensities of 3×10^{14} W/cm^2 and by avoiding laser-beam filamentation typical in low-temperature plasmas. In addition, by directly comparing the power backscattered by SRS from 2 keV plasmas with 3.3 keV plasmas, we find that SRS is efficiently suppressed as the temperature approaches the strong Landau damping regime of a high-electron temperature ignition hohlraum.

The experiments were performed at the Omega laser facility [24]. The plasma is produced by irradiating a cylindrical 2 mm long, 1.6 mm diameter (inner dimensions) gold-hohlraum target (25 μm wall thickness) with a total energy of up to 15 kJ in a 1 ns square pulse, distributed in thirty-seven 351-nm heater beams (Fig. 2). The heater beams irradiate the target symmetrically in three cones on each side (21.4°, 42.0°, and 58.8°) which enter the hohlraum through 800 μm diameter laser entrance holes. The $f/6.7$ beams are pointed at the LEH and are defocused by 1.3 mm (21.4° cone) or 1 mm (42° and 58.8° cones) to reduce the heater laser-beam intensities on the hohlraum wall to 3×10^{14} W/cm^2. Thus, SBS and SRS of the 3ω heater beams are negligible and typically less than 1% of the total heater beam energy. The target is filled with a carbohydrate gas that includes a small amount of Ar dopant (70% C_3H_8, 29% CH_4, 1% Ar by partial pressure). A fill pressure of around 1 atm resulted in a plasma density of $n_e/n_c = 13 \pm 0.3\%$ when fully ionized ($n_c = 4 \times 10^{21}$ cm^{-3} is the critical density for 2ω light). This density is consistent with ignition designs for 2ω light [14]. The LEHs are covered with 260 nm thick polyimide windows to confine the gas inside the hohlraum.

Two-dimensional radiation-hydrodynamic simulations with HYDRA [25], using the experimental beam pointing and focusing, predict peak temperatures in the range of 2–3.5 keV for total heater beam energies of 8–17 kJ [26]. Specifically, for the maximum heater beam energy of 15 kJ applied in this study, a peak temperature of 3.3 keV is obtained along a 2 mm long plateau on the hohlraum axis with a flat profile (Fig. 2). Direct measurements of the plasma conditions with Thomson scattering (TS) have been performed to accurately determine thresholds for laser-plasma interaction instabilities and to predict target performance. We applied an ultraviolet (4ω, 266 nm) probe beam [27] to temporally resolve the electron temperature inside the hohlraum center. The 200 J, 1 ns long probe beam has been focused into the hohlraum along the target axis with a focal spot diameter of 60 μm. Scattered light is collected through a 0.5×0.5 mm^2 polyimide-covered diagnostics window in the hohlraum wall by an $f/10$ lens at an angle of 79° and is imaged onto the slit of a 1 m streaked spectrometer. For our plasma conditions, the scattering parameter is $\alpha = 1/(k_{ia}\lambda_D) \approx 1.6$ and the scattering is collective (k_{ia} is the k vector of the probed ion-acoustic waves and λ_D is the Debye length). The plasma temperature can be accurately determined from a two-ion species fit to the spectrum [Fig. 2(b)] that shows the two ion-acoustic peaks indicating agreement with the hydrodynamic modeling [Fig. 2(c)].

The laser-plasma interactions of a 2ω interaction beam in these hohlraum plasmas has been investigated by measuring the total transmission and backscatter. The 1 ns long flattop interaction beam was delayed by 300 ps relative to the heater beams and had a variable energy of up to 170 J.

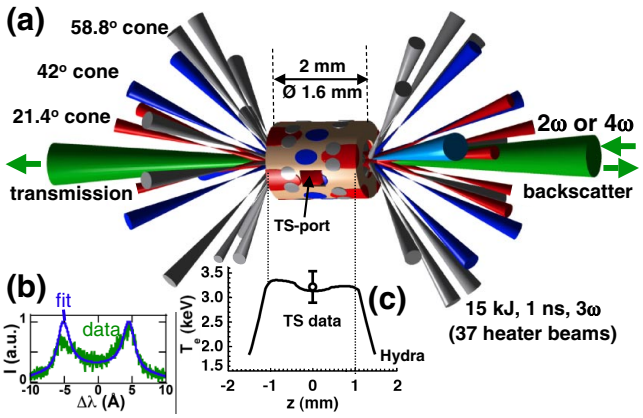

FIG. 2 (color online). The hohlraum target is heated with 37 beams in three cones from each side, delivering a total energy of up to 15 kJ (a). A 2ω interaction beam is fired through the preformed plasma along the hohlraum axis to measure backscatter and propagation. A 4ω probe was alternatively employed for measurements of Thomson scattering (TS) spectra (b) through a 0.5×0.5 mm^2 diagnostics port directly providing plasma temperatures. The TS results compare well to two-dimensional radiation-hydrodynamic simulations with HYDRA that predict a temperature above 3 keV along a 2 mm long plateau on the hohlraum axis (c).

A distributed phase plate (DPP) spatially smoothed the laser beam and produced a Gaussian vacuum spot diameter of 200 μm (full width at half maximum), corresponding to an average intensity of up to 4.7×10^{14} W/cm^2. For some of the experiments, the beam was also temporally smoothed by spectral dispersion [23] adding 3 Å of bandwidth (at 1ω) to the narrow linewidth of the laser to rapidly ($\sim$5 ps) change the speckle pattern of the beam. We further applied PS in some cases, installing a distributed polarization rotator before the final focusing lens to illuminate the target with two distinct and orthogonally polarized speckle patterns.

The transmitted and forward scattered light within twice the original $f/6.7$ cone of the interaction beam has been collected by a high-damage threshold optics inside the target chamber and was sent to a detector assembly outside the chamber. This transmitted beam diagnostic includes absolutely calibrated calorimeters, fast photomultiplier, and fiber-coupled streaked spectrometers. Light scattered directly back into the final focusing lens is collected by the full aperture backscatter station [28] consisting of a pickup wedge that focuses the backscattered light onto a calorimeter and streaked spectrometers that are spectrally filtered for SBS around 527 nm and SRS above 550 nm. The near backscatter imager measures the light that strikes a Lambertian scatter plate surrounding the beam port inside the vacuum chamber. A set of absolutely calibrated, spectrally filtered and time-integrating CCD cameras has been applied determining the absolute backscatter outside the focus lens. Combined, these detectors measure the total forward and backward scattered light with temporal, spectral, and angular resolution [29].

Figure 3(a) shows the streaked spectra of the backscattered and transmitted light. Understanding the frequency shifts of the transmitted and SBS reflected light requires the consideration of two independent processes: In a stationary plasma, the SBS from an ion-acoustic wave in a three-wave parametric instability results in a redshift $\Delta\lambda \approx 2\lambda_{2\omega}(1 - n_e/n_c)^{1/2}C_s/c$ of the reflected light, where C_s is the sound speed, c the light speed, and $\lambda_{2\omega} =$ 527 nm the incident laser wavelength. Light propagating through a plasma whose density is increasing on the time scale of the light transit time experiences a frequency upshift (blueshift) [30,31].

By postprocessing the simulations with gain calculations using the code LIP we find that backscattering occurs at plasma conditions that are consistent with those expected by linear theory for the growth of SBS and SRS [30]. The modeling has also reproduced the observed rapid shift of the transmitted light at 0.7–1.3 ns [Fig. 3(b)] associated with the density change and thus phase velocity change along the laser path during the transit time of the beam. Although the transit time of the laser is only 6 ps for a 2 mm long plasma, the variation in density is sufficient to cause a frequency shift of a few Å [32]. The

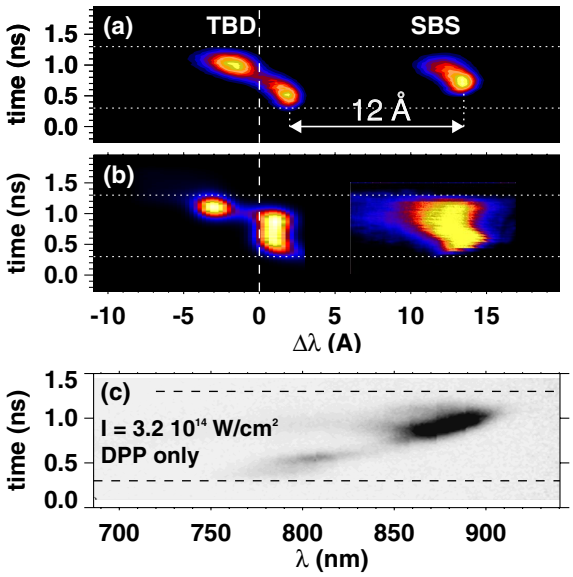

FIG. 3 (color online). Measured spectrum (a) of the transmitted (TBD) and stimulated Brillouin scattered (SBS) light from a 3.3 keV hohlraum plasma and the gain spectrum using HYDRA (b). The relative shift of 12 Å between the transmitted light and SBS is consistent with $T_e \sim 3.3$ keV. The measured SRS peak intensity at around 880 nm (c) is consistent with the plasma density of $n_e/n_c = 13\%$ and indicates that the backscattered light originates from the hot plasma inside the hohlraum.

measured wavelength shifts indicate that the laser-plasma interactions primarily occur within the hot plasma inside the hohlraum.

Figure 4(a) shows the measured integrated transmission of the 2ω beam through the plasma as a function of 2ω beam intensity. We observe a beam transmission approaching 80% at ignition design 2ω laser intensities of 3×10^{14} W/cm^2 and with smoothing by DPP and PS. Additional beam smoothing by SSD has no observable effect in these conditions. Most importantly, with increasing laser intensity, the transmission drops to about 40% for 5×10^{14} W/cm^2 due to a strong increase of SBS reflectivity from 8% to 30% [Fig. 4(b)]. The SRS reflectivity from these high-temperature plasmas is negligible at the 1% level [Fig. 4(c)].

When the heater beam energy into the hohlraum target is reduced from 15 to 8 kJ, the temperature drops from 3.3 to 2 keV and we observe a strong reduction in beam transmission to 25%. Although the SBS reflectivity is observed to drop below 1%, we observe that the measured SRS values increase to about 15%. This behavior at lower temperatures is consistent with open geometry gasbag experiments [20] with the same gasfill, density, and scale length but at peak temperature of only 1.8 keV (open symbols). The maximum beam transmission through gasbag plasmas is only 40% at intensities at 10^{14} W/cm^2 and drops to small levels of 10%–20% at higher intensities.

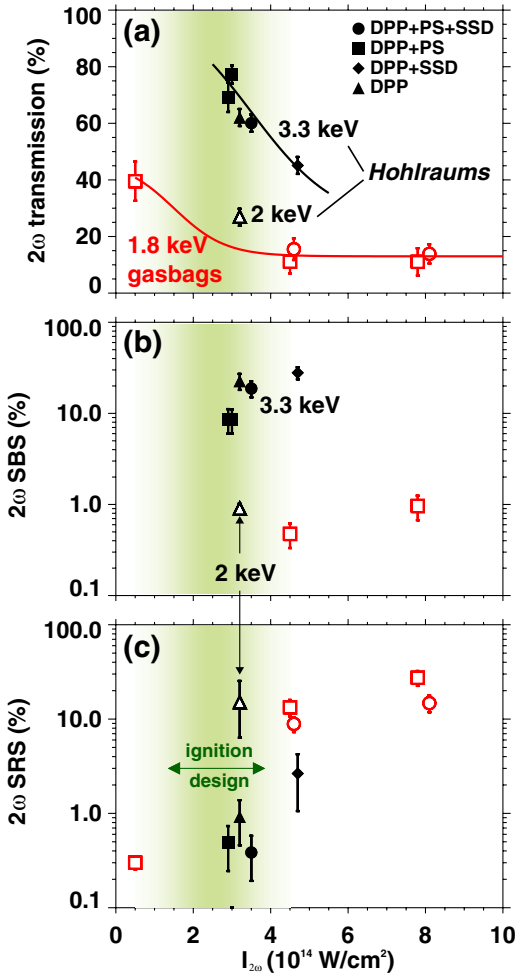

FIG. 4 (color online). Beam transmission (a), SBS reflectivity (b), and SRS reflectivity (c) of the 2ω interaction beam versus beam 2ω intensity for the hohlraum plasmas at temperatures of 3.3 keV (black) and earlier gasbag experiments at 1.8 keV [gray (red)]. The shaded area around 3×10^{14} W/cm^2 indicates the range of intensities used in 2ω ignition designs.

The small transmission values are consistent with the strong inverse bremsstrahlung absorption. Accounting for absorption by both the incident 2ω beam and the backscattered SRS light that becomes energetically important at higher intensities allows us to explain the observations at low temperatures. We note that resonant energy transfer from SRS of the 3ω heater beams is not important at these densities and temperatures [33].

The present results in high-electron temperature plasmas demonstrate the strong suppression of SRS in long scale-length plasmas with increasing electron temperature. The Landau damping rate increases by a factor of 24 from 5×10^{11} to 1.1×10^{13} s^{-1} when increasing the temperature from 1.8 to 3.3 keV; the beam intensity is 3×10^{14} W/cm^2 and density is $n_e/n_{cr} = 0.13$. Thus, the gain rate is reduced from 100 to 10 mm^{-1}.

In summary we present the first measurements of 2ω beam propagation in large scale-length plasmas at ignition design temperatures, laser-beam intensities, and plasma densities. The data show that SRS is efficiently suppressed in high-electron temperature plasmas that approach ignition conditions. In addition, a strong dependence of the reflectivity and transmission on the laser-beam intensity is observed; the measured beam transmission approaching 80% at ignition design intensities of 3×10^{14} W/cm^2 suggest that we can expect good laser energy coupling into ignition targets using green laser beams.

Prepared by LLNL under Contract No. DE-AC52-07NA27344.

[1] J. D. Lindl, Phys. Plasmas **2**, 3933 (1995).
[2] J. D. Lindl *et al.*, Phys. Plasmas **11**, 339 (2004).
[3] S. W. Haan *et al.*, Phys. Plasmas **2**, 2480 (1995).
[4] W. J. Krauser, Phys. Plasmas **3**, 2084 (1996).
[5] L. J. Suter *et al.*, Phys. Rev. Lett. **73**, 2328 (1994); L. J. Suter *et al.*, Phys. Plasmas **3**, 2057 (1996).
[6] R. L. Kauffman *et al.*, Phys. Rev. Lett. **73**, 2320 (1994); R. L. Kauffman *et al.*, Phys. Plasmas **5**, 1927 (1998).
[7] S. H. Glenzer *et al.*, Phys. Rev. Lett. **80**, 2845 (1998); S. H. Glenzer *et al.*, Phys. Plasmas **7**, 2585 (2000).
[8] E. L. Dewald *et al.*, Phys. Rev. Lett. **95**, 215004 (2005).
[9] B. J. MacGowan *et al.*, Phys. Plasmas **3**, 2029 (1996).
[10] D. H. Froula *et al.*, Phys. Rev. Lett. **98**, 085001 (2007).
[11] S. H. Glenzer *et al.*, Nature Phys. **3**, 716 (2007).
[12] M. Stevenson *et al.*, Phys. Plasmas **11**, 2709 (2004).
[13] M. Stevenson *et al.*, Phys. Rev. Lett. **94**, 055006 (2005).
[14] L. J. Suter *et al.*, Phys. Plasmas **11**, 2738 (2004).
[15] C. Labaune, Nature Phys. **3**, 680 (2007).
[16] E. I. Moses and C. R. Wuest, Fusion Sci. Technol. **47**, 314 (2005).
[17] W. L. Kruer, *The Physics of Laser Plasma Interactions* (Addison-Wesley, Reading, MA, 1988).
[18] C. E. Max and K. G. Estabrook, Comments Plasma Phys. Control. Fusion **5**, 239 (1980).
[19] J. D. Moody *et al.*, Phys. Rev. Lett. **86**, 2810 (2001).
[20] C. Niemann *et al.*, Phys. Rev. Lett. **94**, 085005 (2005).
[21] Y. Kato *et al.*, Phys. Rev. Lett. **53**, 1057 (1984).
[22] E. Lefebvre *et al.*, Phys. Plasmas **5**, 2701 (1998).
[23] S. Skupsky *et al.*, J. Appl. Phys. **66**, 3456 (1989).
[24] J. M. Soures *et al.*, Fusion Technol. **30**, 492 (1996).
[25] M. Marinak *et al.*, Phys. Plasmas **5**, 1125 (1998).
[26] D. H. Froula *et al.*, Phys. Plasmas **13**, 052704 (2006).
[27] A. J. Mackinnon *et al.*, Rev. Sci. Instrum. **75**, 3906 (2004).
[28] W. Seka *et al.*, Phys. Rev. Lett. **89**, 175002 (2002).
[29] C. Niemann *et al.*, Rev. Sci. Instrum. **75**, 4171 (2004).
[30] T. Dewandre *et al.*, Phys. Fluids **24**, 528 (1981).
[31] N. B. Meezan *et al.*, Phys. Plasmas **14**, 056304 (2007).
[32] O. L. Landen and W. E. Alley, Phys. Rev. A **46**, 5089 (1992).
[33] R. K. Kirkwood *et al.*, Phys. Rev. Lett. **83**, 2965 (1999).